Two-dimensional Full Particle Simulation of the Flow Patterns in the Scrape-off-layer Plasma for Upper- and Lower- Null Point Divertor Configurations in Tokamaks

T. Takizuka 1), K. Shimizu 1), N. Hayashi 1), M. Hosokawa 2), M. Yagi 3)

1) Japan Atomic Energy Agency, Naka, Japan
2) Research Organization for Information Science & Technology, Tokai, Japan
3) Research Institute for Applied Mechanics, Kyushu University, Kasuga, Japan

e-mail contact of main author: takizuka.tomonori@jaea.go.jp

Abstract. The plasma flow in the scrape-off layer (SOL) plays an important role for the particle control in magnetic fusion reactors. The flow is expected to expel Helium ashes and to retain impurities in the divertor region, if it is directed towards the divertor plate. It has been experimentally observed, however, that the flow direction is sometimes opposite; from the plate side to the SOL middle side in the outer SOL region of tokamaks. A full particle code, PARASOL, is applied to a tokamak plasma with the upper-null-point (UN) or lower-null-point (LN) divertor configuration for the downward ion grad-B drift. PARASOL simulations for the medium aspect ratio reveal the variation of the flow pattern: For the UN case, the flow velocity $V_{//}$ parallel to the magnetic field is directed to the diverter plate both in the inner and outer SOL regions and the stagnation point ($V_{//} = 0$) is located symmetrically at the bottom. On the other hand for the LN case, $V_{//}$ in the outer SOL region has a backward flow pattern. The stagnation point moves below the mid-plane of the outer SOL. These simulation results are very similar to the experimental results. Simulations are carried out by changing the aspect ratio and by artificially cutting the electric field. It is found that the banana motion of trapped ions is very important for the formation of the flow pattern in addition to the self-consistent electric field.

1. Introduction

The plasma flow in the scrape-off layer (SOL) plays an important role for the particle control in magnetic fusion reactors, such as ITER [1]. The flow is expected to expel Helium ashes and to retain impurities in the divertor region, if it is directed towards the divertor plate. It has been experimentally observed, however, that the flow direction is sometimes opposite; from the plate side to the SOL middle side in the outer SOL region (low field side) of tokamaks [2,3]. This backward flow is seen when the single null point is located in the ion ∇B drift direction, while it vanishes for the reversed null-point location. Physics mechanisms of this backward flow have not fully been known, though many simulation studies have been carried out with the fluid model [2,4-6]. Kinetic simulations are considered to bring a breakthrough on this subject [7-9]. Kinetic models are able to simulate the effects of drifts, banana particles, self-consistent electric fields including sheath etc., which are considered to play important roles in the SOL flow formation.

We previously studied the asymmetry of the SOL flow structure in a straight tokamak system by using a particle code PARASOL (PARticle Advanced simulation for SOL and divertor plasmas) [7]. In the present work, we extend the PARASOL to the toroidal system and study the SOL flow patterns in tokamaks. The simulation model of the PARASOL code is described in the next section. Simulation results are presented in Section 3, where the SOL flow patterns in the upper- and lower- null point divertor configurations are demonstrated in comparison with experimental results. Dependence of the flow pattern on the aspect ratio is studied in Section 4. In Section 5, artificial simulations by cutting the electric field are performed to find the major physics factors governing the SOL flow structure. Section 6 consists of summary and discussion.

2. PARASOL Simulation Model

The PARASOL code is fundamentally a time-dependent electrostatic Particle-in-Cell code incorporating a binary collision model [7,10]. The PIC model handles the full particles unlike the δf model that assumes a fixed known background distribution function. The full particle simulation is able to realize a kinetic equilibrium far from the Maxwellian in edge plasmas, although it accompanies the large numerical noise [8]. The PARASOL code has recently been extended to the two-dimensional (2D) toroidal system in the cylindrical coordinates (R, θ, Z) [11]. A tokamak plasma is simulated inside the rectangular region surrounded by walls, $-a_w < R - R_0 < a_w$ and $-b_w < Z < b_w$. All the phenomena studied here are assumed axisymmetric, $\partial/\partial\theta = 0$. The magnetic field $\boldsymbol{B} = (B_R, B_T, B_Z)$ is produced by the combination of a core plasma current channel and two divertor coil currents. The poloidal flux induced by a plasma current channel is simply given as $\Psi \propto -\ln\{a_J^2 + (R-R_0)^2 + (Z/\kappa_J)^2\}$, where a_J , R_0 and κ_J are the minor radius, major radius and elongation of the plasma current channel. By changing the ratio of upper- and lower- divertor coil currents, we have various divertor configurations; upper null (UN), lower null (LN), and double null (DN) configurations. Hereafter, the plasma minor radius a is defined at the mid-plane sparatrix, and the aspect ratio is given as $A = R_0/a$. The toroidal magnetic field B_T is proportional to $1/R$, and the pitch of magnetic field $\Theta \equiv |B_Z/B_T|$ is given at the outer mid-plane separatrix as a small input parameter. Though this magnetic configuration does not satisfy an MHD equilibrium, simulations of electrostatic model can be performed correctly.

We treat a plasma system with single-species ions (mass m_i, and charge e) and electrons (mass m_e, and charge $-e$), for simplicity. Orbits of ions are fully traced, while guiding-center orbits are followed for electrons. The collisionless motion of an ion is described by

$$m_i \, d\boldsymbol{v}/dt = e\,(\boldsymbol{E} + \boldsymbol{v} \times \boldsymbol{B}) + \boldsymbol{F}_c \,, \qquad d\boldsymbol{r}/dt = \boldsymbol{v} \,, \tag{1}$$

where $\boldsymbol{v}$ is the velocity and $\boldsymbol{r}$ is the spatial position. The electric field $\boldsymbol{E}$ is calculated self-consistently with a simple PIC method (see below). In the cylindrical coordinates, a centrifugal force $\boldsymbol{F}_c = m_i\,(v_\theta^2/R, -v_R v_\theta/R, 0)$ arises. It is essential to trace the full ion motion for the correct drift orbit including the polarization drift. On the other hand, the motion of an electron is enough described by the guiding-center equation

$$m_e \, dv_{//}/dt = -\, e\,\boldsymbol{E}\boldsymbol{\cdot}\boldsymbol{B}/B - \mu\,\nabla_{//}B + m_e\, v_{//}\, \boldsymbol{v}_{E\times B}\boldsymbol{\cdot}\boldsymbol{\nabla} B/B \,, \tag{2a}$$

$$d\boldsymbol{r}/dt = v_{//}\,\boldsymbol{B}/B + \boldsymbol{v}_{E\times B} + \boldsymbol{v}_{\nabla B} \,, \tag{2b}$$

where the magnetic moment $\mu \equiv m_e v_\perp^2/2B$ is assumed constant during the collisionless motion. Subscripts // and $\perp$ denote the components parallel to $\boldsymbol{B}$ and perpendicular to $\boldsymbol{B}$, respectively. Major two drift velocities, $\boldsymbol{v}_{E\times B} = (\boldsymbol{E} \times \boldsymbol{B})/B^2$ and $\boldsymbol{v}_{\nabla B} = (m_e/2eB^3)\,(2v_{//}^2 + v_\perp^2)\,(\boldsymbol{\nabla} B \times \boldsymbol{B})$, are taken into account. Equation (1) is advanced in time with a finite time step Δt by using a leap-frog method and Eq. (2) by a predictor-corrector method.

The anomalous transport is simulated with a Monte-Carlo random-walk model. A spatial displacement perpendicular to $\boldsymbol{B}$, $\Delta\boldsymbol{r}_{anom}$, is added for every time step after the motion described by Eqs. (1) and (2). The displacement is given by a Gaussian random number, and its mean square is $<\Delta\mathbf{r}^2_{anom}> = 2\,D_{anom}\,\Delta t$, where D_{anom} is the anomalous diffusion coefficient and is set constant in this study. The anomalous heat transport is incident to this particle diffusion.

Effects of Coulomb collisions are simulated by using a binary collision model [12]. The change in the velocities due to collisions is added after computing the collisionless motion. Major procedures of the model are as follows. (1) In a time interval Δt, a particle in a cell suffers binary collisions with an ion and an electron, which are chosen randomly in the same cell. (2) Change in the relative velocity between colliding pair particles results from a coulomb interaction. Keeping the relative speed, the scattering angle is given as a Gaussian random number. Total momentum and total energy are conserved intrinsically. This model describes the Landau collision integral, while the computation time is linearly proportional to the particle number. One of advantages to introduce such a collision model is to flexibly perform simulations at any arbitrary collisionalities $L_{//}/l_{mfp}$ (ratio of the parallel connection length $L_{//}$ to the mean-free path l_{mfp}). In order to keep the collisionless sheath condition, however, we adopt a "collision cut-off technique" near the wall, because the system size is artificially shortened when it is compared to the sheath width.

An electrostatic part, $\boldsymbol{E}_s = -\nabla\phi$, of the electric field $\boldsymbol{E}$ is determined by Poisson's equation

$$-\nabla^2\phi = (e/\varepsilon_0)\,(n_i - n_e) \tag{3}$$

where ϕ is the electrostatic potential and ε_0 the permittivity of vacuum. Ion and electron densities, n_i and n_e, are calculated self-consistently with a PIC method (see above). The electrostatic potential, including the sheath potential at the plasma-wall boundary, is fully simulated. Although the system size L is very much larger than the Debye length λ_D in real plasmas, PARASOL simulations with the grid size of order of λ_D are available to study such plasmas with smaller values of $L/\lambda_D = 10^2 \sim 10^3$. This is because the characteristics of SOL/ divertor plasmas under the quasi-neutral condition, except in the sheath region, are determined mainly by collisionality $L_{//}/l_{mfp}$ and normalized ion Larmor radius $\rho^* \equiv \rho_i/a$ but insensitive to the L/λ_D value. An inductive part of $\boldsymbol{E}$, such as a toroidal electric field, can be added but is not applied in the present study.

The rectangular wall boundary is considered to be electrically conductive, and the wall potential is set $\phi = 0$. It should be noted that other boundary condition inside the core plasma region is never put artificially. Simulations with this scheme have revealed the variation of potential profiles in tokamak plasmas [11]. As shown in Fig. 1, the ϕ profile changes from convex to concave with the decrease of the aspect ratio A. Even in a straight tokamak (A = 1000), the ϕ profile becomes concave when ρ^* becomes large. If one put an internal boundary condition for ϕ, one can never observe these ϕ profile variations.

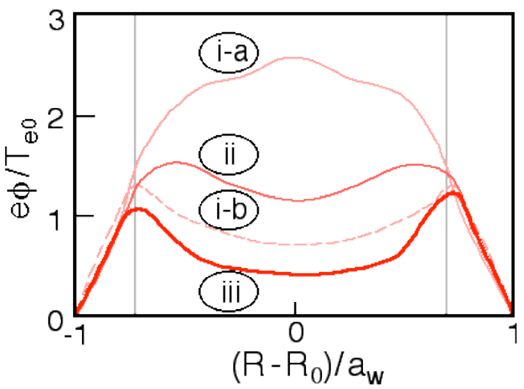

FIG. 1. Potential profiles in tokamaks for various aspect ratio A; (i-a) 1000, (ii) 14 and (iii) 5.5, with ρ^* = 0.022. Large ρ^* makes ϕ profile concave even for straight tokamak (i-b) A = 1000 and ρ^* = 0.062.

Hot particle source is put in the core plasma, and recycling cold particle sources are put near divertor plates. In the present study, the hot source is given uniformly in the core region of $r < 0.9a$ surrounded by a magnetic surface. Ions and electrons with a temperature $T_{i0} = T_{e0} = T_0$ are supplied uniformly in this region. A pair of an ion and an electron is born at the same position. The recycling cold source is neglected in the present paper for simplicity. Particle motions are traced in the whole space inside the vessel. Ions and electrons are diffused out from the core region to the SOL region, and flow into divertor plates. When an ion is lost to the plate, soon at the next time stem a pair of an ion and an electron is supplied in the hot source region. A steady state is finally obtained after a sufficiently long computation.

The number of simulation ions N_i is 10^6 and the number of spatial grids $M_R \times M_Z$ are 320×512. The mass ratio m_i/m_e is chosen as 400 to save the computation time. The pitch of magnetic field Θ is set 0.2 at the outer mid-plane separatrix, i.e., the parallel connection length $L_{//} \sim 2\pi a/\Theta$ is fixed while the safety factor is not fixed during the variation of the aspect ratio A. The normalized ion Larmor radius ρ_i/a is ~ 0.02, the collisionality $L_{//}/l_{mfp}$ is ~ 1, and the normalized diffusion coefficient D_{anom}/aC_s is ~ 10^{-5} (C_s is sound speed).

A parallel computer SGI Altix 3700Bx2 (Intel Itanium2/1.6GHz) is used for PARASOL simulations. A domain decomposition method is applied in the R direction. The computation time of a run is about 12 h with 64 processors.

3. SOL Flow Patterns in the UN and LN Configurations

Flow patterns in the SOL plasma are investigated with PARASOL simulations. A tokamak plasma is confined in a divertor configuration, such as a LN configuration in Fig. 2(a). The hot source is given uniformly in the core region of $r < 0.9a$. Hot particles are diffused out to the SOL region and flow into divertor plates. The steady-state density profile shown in Fig. 2(b) becomes almost parabolic as is analytically evaluated; a solution to the diffusion equation, $(1/r)\,d(rD_{anom}\,dn/dr) = -S$, is $n(r) = \{n(0) - n(a)\}\{1 - (r/a)^2\} + n(a)$. The profiles of electron and ion temperatures are rather flat in the core region, $T_e \approx T_i \approx T_0$ due to the wide hot source region. In the SOL region, T_e decreases sharply, while T_i is still broadened.

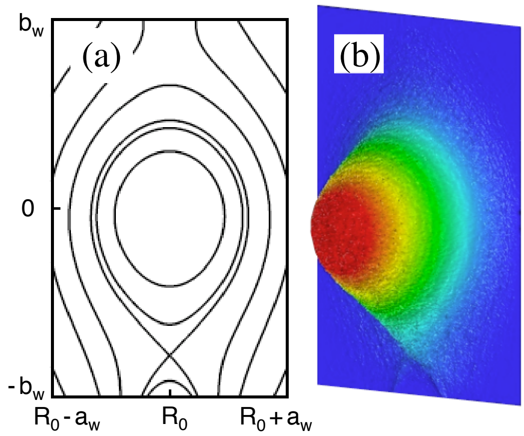

FIG. 2. Magnetic configuration with lower null point. Density profile is shown in (b).

Figure 3 shows the SOL flow patterns for (a) UN configuration and (b) LN configuration, where the ion ∇B drift is downward. The aspect ratio A is about 5.5. For the UN case, the plasma flow velocity $V_{//}$ parallel to B is directed to the diverter plate both in the inner (high-field-side) and outer (low-field-side) SOL regions and the stagnation point ($V_{//} = 0$) is located symmetrically at the bottom. On the other hand for the LN case, $V_{//}$ in the outer SOL region has a backward flow pattern. The stagnation point moves below the mid-plane of the outer

SOL. It is noted that an island of the backward flow is observed in the inner SOL near the separatrix. These simulation results are very similar to the experimental results. In Fig, 4, we compare the PARASOL results and the Alcator C-Mod results [3] on the radial profiles of $V_{//}$. Flow directions (including the backward flow near the inner separatrix for LN case) as well as quantitative Mach numbers resemble each other of experiment and simulation.

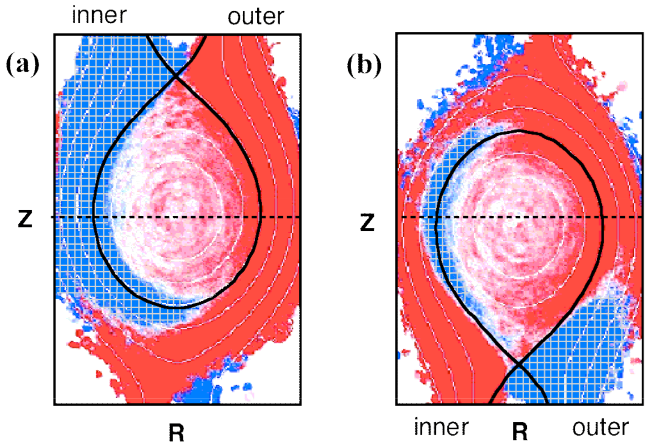

FIG. 3. 2D profile of plasma flow velocity $V_{//}$ parallel to B for (a) UN configuration and (b) LN configuration. Separatrix is drawn by solid black line. Red covered region corresponds to the co-flow to the plasma current (anti-clockwise) and blue meshed region corresponds to the counter-flow (clockwise). The ion ∇B drift is downward. Inner divertor plate is in the left side and outer plate is in the right side for each figure.

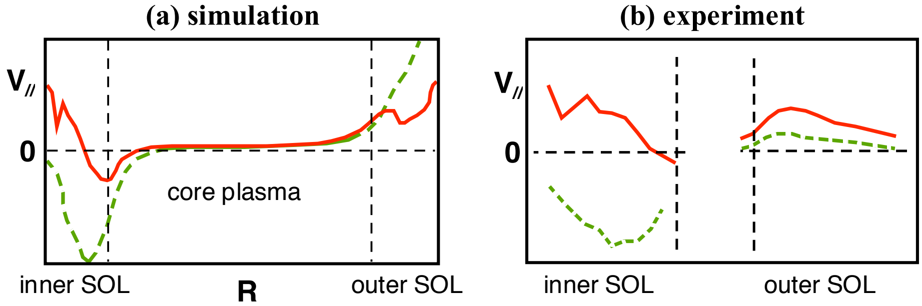

FIG. 4. Radial profiles of $V_{//}$ for UN configuration (dashed green line) and LN configuration (solid red line). Vertical dashed line denotes the position of separatrix. PARASOL simulation results are shown in (a) where the measurement is along the dotted line in Fig. 3. Experimental results of Alcator C-Mod (from Fig, 5 in [3]) are shown in (b) where $V_{//}$ profiles in the inner SOL and the outer SOL are separately plotted. Scales of R and $V_{//}$ are not matched between simulation and experiment.

4. Aspect Ratio Dependence

We study here the toroidal effect on the SOL flow pattern by varying the major radius R_0 (or the aspect ratio $A \equiv R_0/a$). The magnetic field pitch is unchanged to fix the parallel connection length $L_{//} \sim 2\pi a/\Theta$, while the safety factor is changed.

Figure 5 shows the flow patterns for various aspect ratios; A = 5.5, 14 and 1000. The same figures as Fig. 3 reappear for A = 5.5, but the stagnation points ($V_{//}$ = 0) just outside the separatrix are indicated by open arrows. In the UN configuration (upper row in Fig. 5), there exists a single stagnation point. For the medium A (= 5.5) like standard tokamaks, the point is located around the symmetric position (bottom) in the SOL plasma. With the increase of A (= 14), the point is moved to the outer SOL region. In a straight tokamak (A = 1000), the whole SOL flow just outside the separatrix is directed to the inner divertor plate. The stagnation point is located in the outer SOL very near the null point. The reverse flow to the inner plate (counter-flow of blue region) in the outer SOL exists only in a thin layer near the separatrix, and the normal flow toward the outer plate (co-flow of red region) governs the outer SOL region distant from the separatrix. This asymmetric SOL flow structure in a straight tokamak was demonstrated by our previous PARASOL simulation, and the major cause of this structure was clarified to be the flow boundary condition based on the 2D sheath formation [7]. It is noted, therefore, that the symmetric SOL flow structure in standard tokamaks with the UN configuration is created by the toroidal effect.

In the LN configuration (lower row in Fig. 5), the SOL flow structure becomes complex. There are plural stagnation points along the flux tube near the separatrix, for the toroidal geometry, A = 5.5 and 14. For a straight tokamak (A = 1000), the SOL flow structure is perfectly the point-symmetry to the UN case, and there is a single stagnation point. This stagnation point in the inner SOL region near the null point is moved little with the variation of A. The reverse flow to the outer plate (counter-flow of blue region) in the inner SOL region is seen near the separatrix. The radial width of this reverse flow becomes wider for the smaller A. Two stagnation points on either side of a co-flow (red region) appear, and the distance between two points becomes longer for the smaller A.

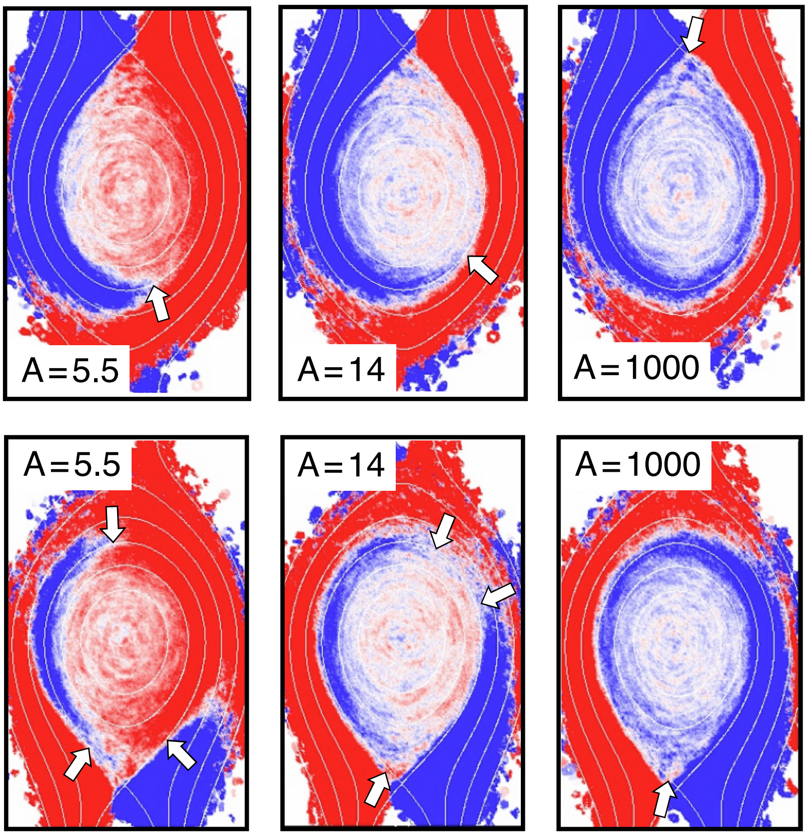

FIG. 5. 2D structures of $V_{//}$ for various aspect ratio A = 5.5, 14 and 1000 in UN configuration (upper row) and LN configuration (lower row). The ion ∇B drift is downward. Red region corresponds to the co-flow (anti-clockwise) and blue region corresponds to the counter-flow (clockwise). Inner divertor plate is in the left side and outer plate is in the right side for each figure. Stagnation points ($V_{//}$ = 0) just outside the separatrix are indicated by open arrows.

5. Artificial Simulations without Electric Field

In order to find the essential factors to form the SOL flow pattern, we carry out the simulations by artificially cutting the electric field E. Collisional interaction between ions and electrons is still taken into account. Results are shown in Fig. 6 in comparison with Fig. 5 for the full simulations. Since the simulation particle number is reduced much, the figures look grainy. The stagnation points for the $E = 0$ simulation are indicated by open arrows, and those for the full simulation by yellow-shaded arrows. In a straight tokamak (A = 1000), the SOL flow structure is completely symmetric when the electric field is absent and ions flow to both divertor plates symmetrically. The change in the position of stagnation point is very large; near the null point for the full simulation and at the opposite side of symmetric position for the $E = 0$ simulation. As the aspect ratio decreases, the change in the stagnation-point position becomes smaller regardless of the UN and LN configurations.

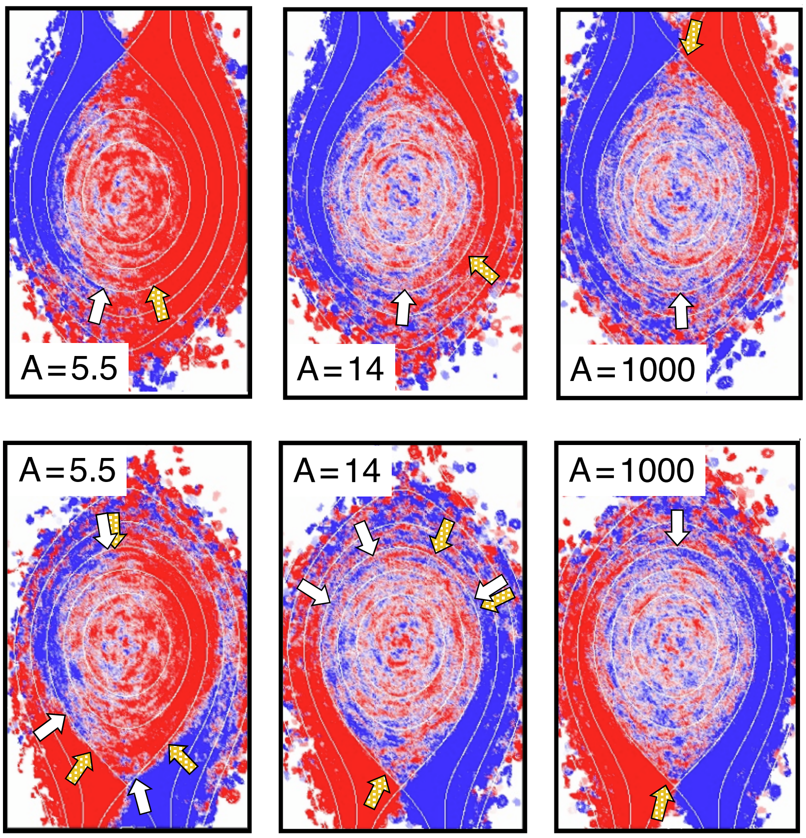

FIG. 6. Results of artificial simulations without electric field. Flow patterns are determined by the ion motions. Configurations are the same as those in Fig. 5. Stagnation points ($V_{//}$ = 0) just outside the separatrix for the E = 0 simulation are indicated by open arrows, and those for the full simulation by yellow-shaded arrows.

In the artificial simulation w/o E, the plasma flow is determined only by ion motions. The ion motions are classified into two kinds, one is the transit motion and the other is the magnetically trapped motion. The transit motion is almost symmetric in the co- and counter directions. On the other hand, the trapped motion causes the asymmetry in the flow direction. The bootstrap-flow effect due to the finite banana width and the orbit loss effect in the edge plasma are important; to which plate trapped ions are lost. We infer that the banana motion of trapped ions is essential for the formation of the flow pattern in addition to the self-consistent electric field. The effect of trapped ions can be stronger than the effect of electric fields for the standard tokamaks with $A < 5$.

5. Summary and Discussion

Complex patterns of the SOL flow in tokamak plasmas are studied with a 2D full particle code PARASOL. The simulations for the medium aspect ratio (A = 5.5) reveal the variation of the flow pattern: In the UN configuration for the downward ion ∇B drift, the flow velocity $V_{//}$ parallel to $\boldsymbol{B}$ is directed to the diverter plate both in the inner and outer SOL regions and the stagnation point ($V_{//}$ = 0) is located symmetrically at the bottom. On the other hand for the LN configuration, $V_{//}$ in the outer SOL region has a backward flow pattern. The stagnation point moves below the mid-plane of the outer SOL. These simulation results are very similar to the experimental results of Alcator C-Mod. The aspect ratio dependence of the SOL flow pattern is investigated. Artificial simulations without the electric field E are carried out in parallel. The change in the flow patterns for the full simulation and the E = 0 simulation is remarkable at the large A, while it becomes less at the smaller A. It is found that the banana motion of trapped ions is very important for the formation of the flow pattern in addition to the self-consistent electric field.

Although the present results of PARASOL simulations realize the SOL flow patterns similar to the experiments, parametric dependences, such as collisionality and recycling, have to be studied in future. Based on the PARASOL simulation results, it is required to develop a model of the trapped-ion induced flow in the edge plasma for the comprehensive divertor simulation with the fluid model.

Acknowledgments

The authors thank Dr. N. Asakura for his valuable information and discussion about the experiments of the SOL flows. This work was partly supported by the Grant-in-Aid for Scientific Research of Japan Society for the Promotion of Science.

References

[1] Progress in the ITER Physics Basis: Chapter 4, Nucl. Fusion **47** (2007) S203.
[2] ASAKURA, N., ITPA SOL and Divertor Topical Group, J. Nucl. Mater. **363-365** (2007) 41.
[3] LABOMBARD, B., et al, Nucl. Fusion **44** (2004) 1047.
[4] PITTS, R., et al, J. Nucl. Mater. **337-339** (2005) 146.
[5] HOSHINO, K., et al, J. Nucl. Mater. **363-365** (2007) 539.
[6] PIGAROV, A.Y., et al., Contrib. Plasma Phys. **48** (2008) 82.
[7] TAKIZUKA, T., HOSOKAWA, M., SHIMIZU, K., J. Nucl. Mater. **313-316** (2003) 1331.
[8] CHANG, C.S., KU, S., WEITZNER, H., Phys. Plasmas **11** (2004) 2649;
CHANG, C.S., KU, S., Phys. Plasmas **15** (2008) 062510.
[9] COHEN, R., XU, X.Q., Contrib. Plasma Phys. **48** (2008) 212.
[10] TAKIZUKA, T., HOSOKAWA, M., SHIMIZU, K., Trans. Fusion Technol. **39** (2001) 111.
[11] TAKIZUKA, T., HOSOKAWA, M., "Two-dimensional Full Particle Simulation of the Formation of Electrostatic Field in a Tokamak Plasma", 11th IAEA Technical Meeting on H-mode Physics and Transport Barriers, Tsukuba, 2007.
[12] TAKIZUKA, T., ABE, H., J. Comput. Phys. **25** (1977) 205.